

2008

Ratios of $^{15}\text{N}/^{12}\text{C}$ and $^4\text{He}/^{12}\text{C}$ Inclusive Electroproduction Cross Sections in the Nucleon Resonance Region

P. E. Bosted

R. Fersch

G. Adams

M. Amaryan

Old Dominion University

S. Anefalos

See next page for additional authors

Follow this and additional works at: https://digitalcommons.odu.edu/physics_fac_pubs

 Part of the [Nuclear Commons](#)

Repository Citation

Bosted, P. E.; Fersch, R.; Adams, G.; Amaryan, M.; Anefalos, S.; Anghinolfi, M.; Asryan, G.; Avakian, H.; Badasaryan, H.; Baillie, N.; Bektasoglu, M.; Bültmann, S.; Careccia, S. L.; Dodge, G. E.; Dharmawardane, K. V.; Forest, T. A.; Gavalian, G.; Guler, N.; Hyde-Wright, C. E.; Kalantarians, N.; Klein, A.; Kuhn, S. E.; Lachniet, J.; Niyazov, R. A.; Qin, L. M.; Sabatié, F.; Tkachenko, S.; Weinstein, L. B.; and Zhang, J., "Ratios of $^{15}\text{N}/^{12}\text{C}$ and $^4\text{He}/^{12}\text{C}$ Inclusive Electroproduction Cross Sections in the Nucleon Resonance Region" (2008). *Physics Faculty Publications*. 90.
https://digitalcommons.odu.edu/physics_fac_pubs/90

Original Publication Citation

Bosted, P. E., Fersch, R., Adams, G., Amaryan, M., Anefalos, S., Anghinolfi, M., . . . Zhao, Z. (2008). Ratios of $^{15}\text{N}/^{12}\text{C}$ and $^4\text{He}/^{12}\text{C}$ inclusive electroproduction cross sections in the nucleon resonance region. *Physical Review C*, 78(1), 015202. doi:10.1103/PhysRevC.78.015202

Authors

P. E. Bosted, R. Fersch, G. Adams, M. Amaryan, S. Anefalos, M. Anghinolfi, G. Asryan, H. Avakian, H. Badasaryan, N. Baillie, M. Bektasoglu, S. Bültmann, S. L. Careccia, G. E. Dodge, K. V. Dharmawardane, T. A. Forest, G. Gavalian, N. Guler, C. E. Hyde-Wright, N. Kalantarians, A. Klein, S. E. Kuhn, J. Lachniet, R. A. Niyazov, L. M. Qin, F. Sabatié, S. Tkachenko, L. B. Weinstein, and J. Zhang

Ratios of $^{15}\text{N}/^{12}\text{C}$ and $^4\text{He}/^{12}\text{C}$ inclusive electroproduction cross sections in the nucleon resonance region

P. E. Bosted,^{35,*} R. Fersch,³⁹ G. Adams,³¹ M. Amarian,²⁹ S. Anefalos,¹⁷ M. Anghinolfi,¹⁸ G. Asryan,⁴⁰ H. Avakian,^{17,35} H. Bagdasaryan,^{29,40} N. Baillie,³⁹ J. P. Ball,² N. A. Baltzell,³⁴ S. Barrow,¹³ V. Batourine,³⁵ M. Battaglieri,¹⁸ K. Beard,²¹ I. Bedlinskiy,²⁰ M. Bektasoglu,²⁹ M. Bellis,^{5,31} N. Benmouna,¹⁴ A. S. Biselli,¹¹ B. E. Bonner,³² S. Bouchigny,^{19,35} S. Boiarinov,^{20,35} R. Bradford,⁵ D. Branford,¹⁰ W. K. Brooks,³⁵ S. Bültmann,²⁹ V. D. Burkert,³⁵ C. Butuceanu,³⁹ J. R. Calarco,²⁶ S. L. Careccia,²⁹ D. S. Carman,³⁵ B. Carnahan,⁶ A. Cazes,³⁴ S. Chen,¹³ P. L. Cole,^{16,35} P. Collins,² P. Coltharp,¹³ D. Cords,^{35,†} P. Corvisiero,¹⁸ D. Crabb,³⁸ H. Crannell,⁶ V. Crede,¹³ J. P. Cummings,³¹ R. De Masi,⁷ R. De Vita,¹⁸ E. De Sanctis,¹⁷ P. V. Degtyarenko,³⁵ H. Denizli,³⁰ L. Dennis,¹³ A. Deur,³⁵ C. Djalali,³⁴ G. E. Dodge,²⁹ J. Donnelly,¹⁵ D. Dougherty,^{8,35} P. Dragovitsch,¹³ M. Dugger,² K. V. Dharmawardane,^{29,‡} S. Dytman,³⁰ O. P. Dzyubak,³⁴ H. Egiyan,^{35,39,§} K. S. Egiyan,^{40,‡} L. Elouadrhiri,^{8,35} P. Eugenio,¹³ R. Fatemi,³⁸ G. Fedotov,²⁵ R. J. Feuerbach,⁵ T. A. Forest,²⁹ A. Fradi,¹⁹ H. Funsten,³⁹ M. Garçon,⁷ G. Gavalian,^{26,29} G. P. Gilfoyle,³³ K. L. Giovanetti,²¹ F. X. Girod,⁷ J. T. Goetz,³ E. Golovatch,^{18,||} R. W. Gothe,³⁴ K. A. Griffioen,³⁹ M. Guidal,¹⁹ M. Guillo,³⁴ N. Guler,²⁹ L. Guo,³⁵ V. Gyurjyan,³⁵ C. Hadjidakis,¹⁹ K. Hafidi,¹ R. S. Hakobyan,⁶ J. Hardie,^{8,35} D. Heddle,^{8,35} F. W. Hersman,²⁶ K. Hicks,²⁸ I. Hleiqawi,²⁸ M. Holtrop,²⁶ M. Huertas,³⁴ C. E. Hyde-Wright,²⁹ Y. Ilieva,¹⁴ D. G. Ireland,¹⁵ B. S. Ishkhanov,²⁵ E. L. Isupov,²⁵ M. M. Ito,³⁵ D. Jenkins,³⁷ H. S. Jo,¹⁹ K. Joo,⁹ H. G. Juengst,²⁹ N. Kalantarians,²⁹ C. Keith,³⁵ J. D. Kellie,¹⁵ M. Khandaker,²⁷ K. Y. Kim,³⁰ K. Kim,²² W. Kim,²² A. Klein,^{29,¶} F. J. Klein,^{6,12} M. Klusman,³¹ M. Kossov,²⁰ L. H. Kramer,^{12,35} V. Kubarovskiy,^{31,35} J. Kuhn,^{5,31} S. E. Kuhn,²⁹ S. V. Kuleshov,²⁰ J. Lachniet,^{5,29} J. M. Laget,^{7,35} J. Langheinrich,³⁴ D. Lawrence,²⁴ Ji Li,³¹ A. C. S. Lima,¹⁴ K. Livingston,¹⁵ H. Lu,³⁴ K. Lukashin,⁶ M. MacCormick,¹⁹ N. Markov,⁹ S. McAleer,¹³ B. McKinnon,¹⁵ J. W. C. McNabb,⁵ B. A. Mecking,³⁵ M. D. Mestayer,³⁵ C. A. Meyer,⁵ T. Mibe,²⁸ K. Mikhailov,²⁰ R. Minehart,³⁸ M. Mirazita,¹⁷ R. Miskimen,²⁴ V. Mokeev,²⁵ L. Morand,⁷ S. A. Morrow,^{7,19} M. Moteabbed,¹² J. Mueller,³⁰ G. S. Mutchler,³² P. Nadel-Turonski,¹⁴ R. Nasseripour,^{12,34} S. Niccolai,^{14,19} G. Niculescu,²¹ I. Niculescu,^{14,21} B. B. Niczyporuk,³⁵ M. R. Niroula,²⁹ R. A. Niyazov,^{29,35} M. Nozar,³⁵ G. V. O'Rielly,¹⁴ M. Osipenko,^{18,25} A. I. Ostrovidov,¹³ K. Park,²² E. Pasyuk,² C. Paterson,¹⁵ S. A. Philips,¹⁴ J. Pierce,³⁸ N. Pivnyuk,²⁰ D. Pocanic,³⁸ O. Pogorelko,²⁰ E. Polli,¹⁷ S. Pozdniakov,²⁰ B. M. Preedom,³⁴ J. W. Price,⁴ Y. Prok,^{38,**} D. Protopopescu,^{15,26} L. M. Qin,²⁹ B. A. Raue,^{12,35} G. Riccardi,¹³ G. Ricco,¹⁸ M. Ripani,¹⁸ G. Rosner,¹⁷ P. Rossi,¹⁷ D. Rowntree,²³ P. D. Rubin,³³ F. Sabatié,^{7,29} C. Salgado,²⁷ J. P. Santoro,^{35,37,††} V. Sapunenko,^{18,35} R. A. Schumacher,⁵ V. S. Serov,²⁰ Y. G. Sharabian,³⁵ J. Shaw,²⁴ N. V. Shvedunov,²⁵ A. V. Skabelin,²³ E. S. Smith,³⁵ L. C. Smith,³⁸ D. I. Sober,⁶ A. Stavinsky,²⁰ S. S. Stepanyan,²² S. Stepanyan,^{8,35,40} B. E. Stokes,¹³ P. Stoler,³¹ S. Strauch,³⁴ R. Suleiman,²³ M. Taiuti,¹⁸ S. Taylor,³² D. J. Tedeschi,³⁴ U. Thoma,^{35,‡‡} A. Tkabladze,¹⁴ S. Tkachenko,²⁹ L. Todor,⁵ M. Ungaro,⁹ M. F. Vineyard,^{33,36} A. V. Vlassov,²⁰ L. B. Weinstein,²⁹ D. P. Weygand,³⁵ M. Williams,⁵ E. Wolin,³⁵ M. H. Wood,^{34,§§} A. Yegneswaran,³⁵ J. Yun,²⁹ L. Zana,²⁶ J. Zhang,²⁹ B. Zhao,⁹ and Z. Zhao³⁴

(CLAS Collaboration)

¹Argonne National Laboratory, Argonne, Illinois 60439, USA

²Arizona State University, Tempe, Arizona 85287-1504, USA

³University of California at Los Angeles, Los Angeles, California 90095-1547, USA

⁴California State University, Dominguez Hills, Carson, California 90747, USA

⁵Carnegie Mellon University, Pittsburgh, Pennsylvania 15213, USA

⁶Catholic University of America, Washington, D.C. 20064, USA

⁷CEA-Saclay, Service de Physique Nucléaire, F-91191 Gif-sur-Yvette, France

⁸Christopher Newport University, Newport News, Virginia 23606, USA

⁹University of Connecticut, Storrs, Connecticut 06269, USA

¹⁰Edinburgh University, Edinburgh EH9 3JZ, United Kingdom

¹¹Fairfield University, Fairfield, Connecticut 06824, USA

¹²Florida International University, Miami, Florida 33199, USA

¹³Florida State University, Tallahassee, Florida 32306, USA

¹⁴George Washington University, Washington, D.C. 20052, USA

¹⁵University of Glasgow, Glasgow G12 8QQ, United Kingdom

¹⁶Idaho State University, Pocatello, Idaho 83209, USA

¹⁷INFN, Laboratori Nazionali di Frascati, I-00044 Frascati, Italy

¹⁸INFN, Sezione di Genova, I-16146 Genova, Italy

¹⁹Institut de Physique Nucleaire ORSAY, Orsay, France

²⁰Institute of Theoretical and Experimental Physics, RU-117259 Moscow, Russia

²¹James Madison University, Harrisonburg, Virginia 22807, USA

²²Kyungpook National University, Daegu 702-701, South Korea

²³Massachusetts Institute of Technology, Cambridge, Massachusetts 02139-4307, USA

²⁴University of Massachusetts, Amherst, Massachusetts 01003, USA

²⁵Moscow State University, General Nuclear Physics Institute, RU-119899 Moscow, Russia

²⁶*University of New Hampshire, Durham, New Hampshire 03824-3568, USA*²⁷*Norfolk State University, Norfolk, Virginia 23504, USA*²⁸*Ohio University, Athens, Ohio 45701, USA*²⁹*Old Dominion University, Norfolk, Virginia 23529, USA*³⁰*University of Pittsburgh, Pittsburgh, Pennsylvania 15260, USA*³¹*Rensselaer Polytechnic Institute, Troy, New York 12180-3590, USA*³²*Rice University, Houston, Texas 77005-1892, USA*³³*University of Richmond, Richmond, Virginia 23173, USA*³⁴*University of South Carolina, Columbia, South Carolina 29208, USA*³⁵*Thomas Jefferson National Accelerator Facility, Newport News, Virginia 23606, USA*³⁶*Union College, Schenectady, New York 12308, USA*³⁷*Virginia Polytechnic Institute and State University, Blacksburg, Virginia 24061-0435, USA*³⁸*University of Virginia, Charlottesville, Virginia 22901, USA*³⁹*College of William and Mary, Williamsburg, Virginia 23187-8795, USA*⁴⁰*Yerevan Physics Institute, 375036 Yerevan, Armenia*

(Received 17 December 2007; revised manuscript received 13 April 2008; published 11 July 2008)

The (W , Q^2) dependence of the ratio of inclusive electron scattering cross sections for $^{15}\text{N}/^{12}\text{C}$ was determined in the kinematic ranges $0.8 < W < 2$ GeV and $0.2 < Q^2 < 1$ GeV² using 2.285 GeV electrons and the CLAS detector at Jefferson Lab. The ratios exhibit only slight resonance structure, in agreement with a simple phenomenological model and an extrapolation of deep-inelastic scattering ratios to low Q^2 . Ratios of $^4\text{He}/^{12}\text{C}$ using 1.6 to 2.5 GeV electrons were measured with very high statistical precision and were used to correct for He in the N and C targets. The (W , Q^2) dependence of the $^4\text{He}/^{12}\text{C}$ ratios is in good agreement with that of the phenomenological model and exhibit significant resonance structure centered at $W = 0.94$, 1.23, and 1.5 GeV.

DOI: [10.1103/PhysRevC.78.015202](https://doi.org/10.1103/PhysRevC.78.015202)

PACS number(s): 25.30.Fj, 13.60.Hb, 14.20.Gk, 27.20.+n

I. INTRODUCTION

While the internal structure of the proton has received enormous attention over the past decades, the structure of its isospin partner, the neutron, has not been studied as intensively. The response of the neutron to electromagnetic probes is not only of interest to characterize the structure of the nucleon but also is of considerable practical application, in particular when the neutron is embedded in a nucleus.

The application that motivated the present study is the need to understand the cross sections for electron scattering from ^{15}N in experiments using ammonia ($^{15}\text{NH}_3$ or $^{15}\text{ND}_3$) as a

source of polarized protons or deuterons. In experiments using polarized ammonia to measure the spin structure functions g_1 and g_2 , data are also taken using a carbon target, so that in practice the “dilution” from unpolarized materials (i.e., relative ratio of counts from ^{15}N) can be determined from good fits to the ratios $^{15}\text{N}/^{12}\text{C}$ and measured ratios of carbon to proton or deuteron cross sections. Polarized ammonia targets are normally immersed in a bath of liquid He, so it is also important to study $^4\text{He}/^{12}\text{C}$.

Another area where precision knowledge of the differences in proton and neutron structure is of increasing practical importance is in the field of neutrino scattering. The targets in these low-rate experiments are normally made of heavy materials such as iron to maximize count rates. The structure of the neutron in iron has already been shown to be important to the interpretation of the NuTeV experiment [1]. Precision knowledge of lepton-nucleon scattering from nuclei will be of particular importance to the interpretation of planned neutrino oscillation experiments [2].

A considerable body of data [3] for inelastic lepton-nucleon scattering from nuclei exists for a variety of nuclei in the deep-inelastic scattering (DIS) region (missing mass $W > 2$ GeV, 4-momentum transfer $Q^2 > 1$ GeV²), where one expects the n/p ratio in a nucleus to be very similar to that determined from d/p ratios. For $W < 2$ GeV, the effects of prominent nucleon resonances, nucleon Fermi motion, Meson Exchange Currents (MEC), and Final State Interactions (FSI) in larger nuclei are of greater magnitude than those in the case of deuterium, so one can no longer simply use d/p ratios to account for the neutron excess in nuclei such as ^{15}N or Fe. Comparisons of nuclei with similar atomic numbers, but differing ratios of neutrons to

*bosted@jlab.org; corresponding author.

†Deceased

‡Current address: Thomas Jefferson National Accelerator Facility, Newport News, Virginia 23606, USA.

§Current address: University of New Hampshire, Durham, New Hampshire 03824-3568, USA.

||Current address: Moscow State University, General Nuclear Physics Institute, 119899 Moscow, Russia.

¶Current address: Los Alamos National Laboratory, Los Alamos, New Mexico 87545, USA.

**Current address: Massachusetts Institute of Technology, Cambridge, Massachusetts 02139-4307, USA.

††Current address: Catholic University of America, Washington, D.C. 20064, USA.

‡‡Current address: Physikalisches Institut der Universität Giessen, 35392 Giessen, Germany.

§§Current address: University of Massachusetts, Amherst, Massachusetts 01003, USA.

TABLE I. Mass thickness t_m and percentage of radiation length (r.l.) t_r of materials in each of the targets used in this experiment.

Material	Targets	t_m (g/cm ²)	t_r (r.l.)
^{12}C	C	0.501 ± 0.005	1.17%
^{15}N	N	0.56 ± 0.03	1.4%
^4He	C, N, MT	0.25 ± 0.01	0.2%
Al	C, N, MT	0.045 ± 0.002	0.018%
Kapton	C, N, MT	0.072 ± 0.002	0.017%

protons, are relatively few in the nucleon resonance region [4]. The measurements of $^{15}\text{N}/^{12}\text{C}$ over a wide range of (W , Q^2) in the nucleon resonance region from the present experiment were designed to help address this situation. An interesting by-product is a large body of high statistical precision ratios of $^4\text{He}/^{12}\text{C}$ with a common systematic error.

II. EXPERIMENT

The present results were obtained as part of the Eg1b experiment [5] at Jefferson Lab, conducted in 2001. The bulk of the experiment used polarized ammonia targets [6] to study electron scattering from polarized hydrogen and deuterium. The ammonia content was dominated by ^{15}N and was bathed in liquid He. Therefore, we measured scattering from solid ^{15}N , carbon, and empty targets, all bathed in liquid He, to understand and account for the unpolarized ‘‘dilution factor.’’ This article reports on the results obtained with a 2.285 GeV electron beam for the nitrogen to carbon ratios and beam energies of 1.603, 1.721, and 2.285 GeV for the empty to carbon target ratios.

Electrons scattered at angles between 10° and 45° were detected in CLAS [7]. Experimental targets for ^{15}N and ^{12}C data consisted of frozen ^{15}N material inside a thin (~ 1.7 cm) target cup and an amorphous carbon slab, respectively. Both were immersed in an approximately 1.7-cm-long, 1 K LHe bath between two thin aluminum and Kapton windows. The vertex tracking resolution was not sufficiently precise to distinguish between events scattering from the windows, the LHe bath, or the central nitrogen and carbon targets. A third target (MT) contained only LHe and the thin windows. The mass thicknesses of all target materials are listed in Table I. For modeling purposes, Kapton is approximated as equivalent to ^{12}C . While the thickness of the carbon slab was relatively well known, the thicknesses of LHe and nitrogen were relatively poorly determined, due to the difficulties of working with targets at 1 K.

Scattered electrons were principally identified (and distinguished from pions) by a Cherenkov threshold detector and electromagnetic shower calorimeter. Their momenta were determined by drift chambers and time-of-flight tracking in a (superconducting torus) magnetic field, with a trigger threshold of 0.3 GeV. Kinematically complete elastic ep and inelastic $ep\pi^+\pi^-$ events from separate NH_3 scattering data were used for calibration of the momentum scale [8]. Additional details on the beam, detectors, calibrations, and data analysis can be found in Ref. [8].

Ratios of count rates, normalized to total (live-time gated) incident electron charge, were calculated for the nitrogen and carbon target scattering events and binned in Q^2 and final state invariant mass W . All $^{15}\text{N}/^{12}\text{C}$ ratios were for a beam energy of 2.285 GeV. Similar ratios were also calculated between the carbon and empty targets, for the determination of the $^{12}\text{C}/^4\text{He}$ cross section ratios. In this case, the ratios at each of three beam energies, 1.603, 1.721, and 2.285 GeV, were taken individually, and the results were then averaged. A χ^2 test showed the three sets of ratios to be statistically compatible. Small corrections were made for pions misidentified as electrons and for electrons from pair-symmetric decays of π^0 mesons (measured by reversing the CLAS torus polarity). Systematic errors in the cross section ratios from these corrections were generally very small, with a maximum of 0.5% at the highest W .

Radiated cross section models accounting for the mass and radiation length thicknesses of all materials within the targets were then fit to the count ratio measurements. The two fit parameters were the thickness of the nitrogen target and the length of the LHe. Internal and external radiative effects were accounted for using the formalism of Mo and Tsai [9]. The treatment of radiative effects required modeling of nuclear elastic, quasielastic, and inelastic cross sections from all nuclei in the targets. The calculations used the nuclear charge radii of Ref. [10] for the elastic form factors (evaluated in the shell model) and the superscaling model of Ref. [11] for the quasielastic cross sections with the nucleon elastic form factor parametrization in Ref. [12] and the y -scaling function of Ref. [13] for both the longitudinal and transverse cross sections. The Donnelly model [11] has two parameters (loosely related to Fermi broadening and average binding energy) that differ from nucleus to nucleus: we used $(k_F, E_s) = (0.170, 0.015)$ GeV for ^4He and $(k_F, E_s) = (0.228, 0.020)$ GeV for carbon and nitrogen. A Pauli-suppression correction at low Q^2 used the prescription of Mo and Tsai [9]. Inelastic scattering was modeled using a Fermi-convolution method of ‘‘smearing’’ free proton [14] and neutron [15] cross sections. The smearing was done in a manner similar to that described for the deuteron in Ref. [15]. A detailed description, with the numerous formulas and parameters involved, is beyond the scope of this article. However, the FORTRAN computer code for both the quasielastic and inelastic models used in this article is available [16]. Systematic errors were determined by making reasonable variations in the cross section models and target parameters.

The contributions from the LHe in the carbon and nitrogen targets were subtracted using the radiated cross section global fit, as were the contributions from the aluminum and Kapton windows in all three targets. Born-level ratios were then determined from the background-subtracted ratios, using the calculated ratio of Born and radiated cross sections for each target material.

III. RESULTS FOR $^4\text{He}/^{12}\text{C}$

The beam-energy averaged ratios of Born-level cross sections for $^4\text{He}/^{12}\text{C}$ are shown as the solid circles in Fig. 1. Numerical results are available in the CLAS database [17]. It

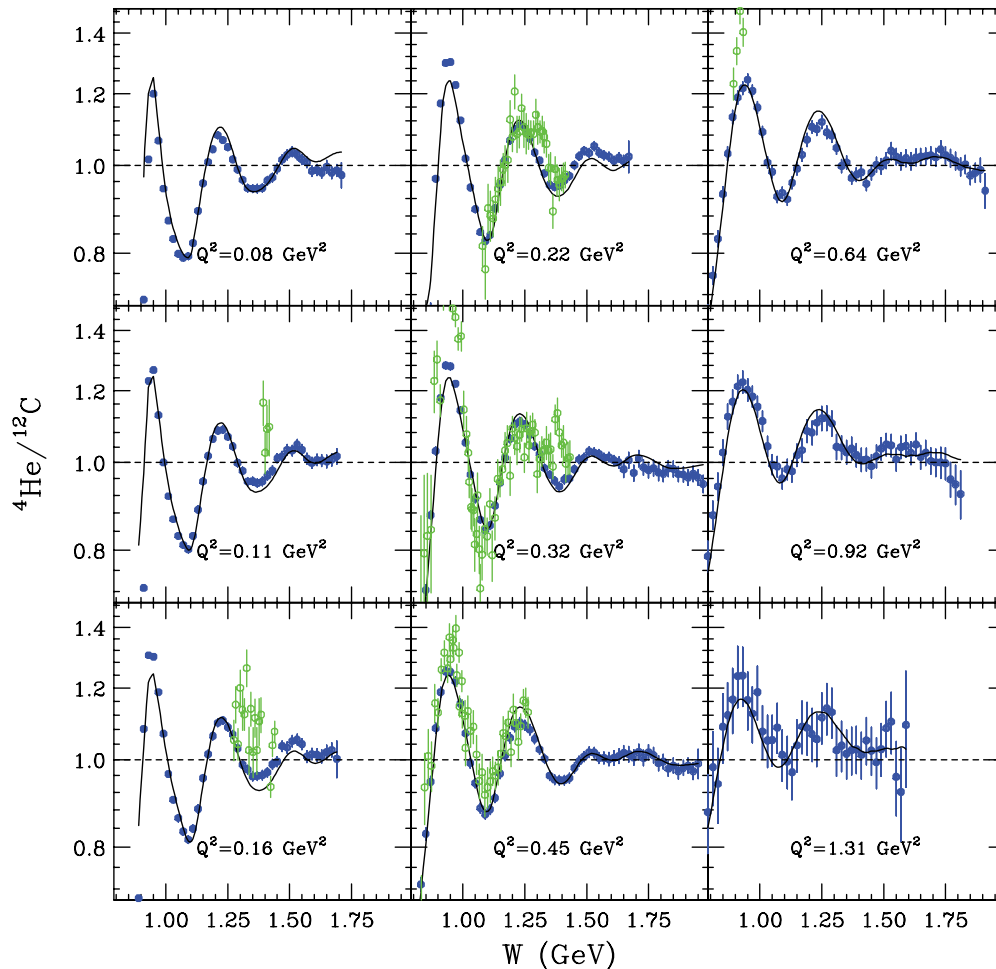


FIG. 1. (Color online) Extracted ratios of ${}^4\text{He}$ to ${}^{12}\text{C}$ cross sections (per nucleon) from this experiment (solid blue circles), using beam energies of 1.6 to 2.2 GeV, showing statistical and point-to-point systematic errors added in quadrature. The overall normalization error is 4%. The solid curves show the ratio of model cross sections. The green open circles are from SLAC Experiment NE5 [18].

can be seen that the results are generally in good agreement with (W, Q^2) dependence of the ratios from the Born-level inelastic cross section model that we used for radiative corrections and background subtractions (solid curves). This validates the use of this model in correcting for the LHe contributions to the carbon and nitrogen targets. At moderate Q^2 , the present ratios are reasonably consistent with previous data taken at a scattering angle of 37° degrees and beam energies of 0.9 to 1.2 GeV at SLAC [18] (open circles). The high statistical precision of the present data is useful for constraining future fits to the kinematic dependence of helium and carbon cross sections. In particular, the widths of the peaks near $W = 0.94$ GeV (from quasielastic scattering) and $W = 1.23$ GeV (from excitation of the $\Delta(1232)$ resonance) are very sensitive to the difference in average Fermi motion between helium and carbon (we used 180 and 225 MeV, respectively, for the Fermi smearing parameter k_F in our model). The depth of the dip between these two peaks is sensitive to possible differences in MEC and FSI (we assumed no difference in our model). A slight peak in the ratios near $W = 1.5$ GeV is also evident in both the data and model at lower values of Q^2 .

IV. RESULTS FOR ${}^{15}\text{N}/{}^{12}\text{C}$

The ratios of extracted Born cross sections per nucleon for ${}^{15}\text{N}/{}^{12}\text{C}$ are plotted in Fig. 2 as a function of invariant mass W for nine bins in Q^2 and a beam energy of 2.285 GeV. Point-to-point systematic errors (included in the outer error bars) are relatively small. Because of the uncertainties in the target material thicknesses, there is an overall normalization error of 6%. Numerical results are available in the CLAS database [17].

In general, there is good agreement with the cross section model ratios used for radiative and background corrections, shown as the solid curves. The pronounced dips in the ratios near the quasielastic region ($W = 0.94$ GeV) “level off” with increasing Q^2 , due to the increasing contributions from inelastic scattering and the increasing ratio of neutron to proton elastic form factors. The ratios in the resonance region ($W > 1.1$ GeV) show only slight resonant structure. At lower Q^2 , both the data and the model show enhanced ratios near the $\Delta(1232)$ peak, where the neutron to proton ratio is expected to approach unity due to the isovector nature of this resonance, while the nonresonant background has a smaller ratio [15]. The enhancement near $W = 1.23$ GeV in the model is not due to a difference in Fermi motion, because the same average

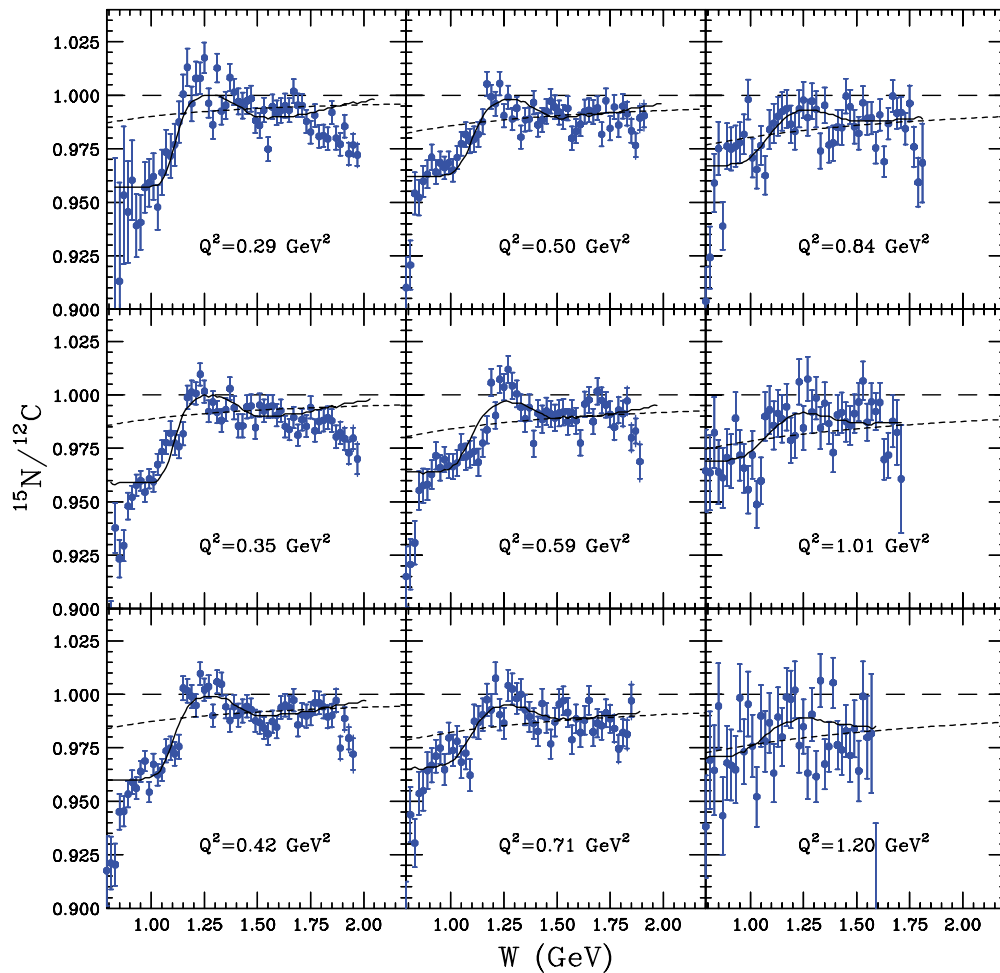


FIG. 2. (Color online) Extracted ratios of cross sections per nucleon for pure ^{15}N to ^{12}C from this experiment (blue solid circles). The inner error bars show statistical errors only, while the outer bars include point-to-point systematic errors added in quadrature. The overall normalization error is 6%. The solid curves show ratios of the model cross sections used for radiative corrections and background subtraction. The dashed curves were generated using $\sigma_n/\sigma_p = (1 - 0.8\xi)$. The long dashed lines are plotted at unity, for reference.

Fermi momentum was assumed in the model for carbon and nitrogen. A slight dip near the $S_{11}(1535)$ resonance is possibly evident. At higher Q^2 , Fermi smearing effects become more significant, and all indications of resonant structure disappear.

On average, the ratios tend to decrease with increasing Q^2 at fixed W , corresponding to larger values of the Bjorken scaling variable x . In deep-inelastic scattering, σ_n/σ_p is approximately given by $(1 - 0.8x)$ [19]. To approximately take into account target-mass effects, x was replaced with the Nachtmann [20] scaling variable $\xi \equiv 2x/(1 + \sqrt{1 + 4M^2x^2/Q^2})$. The dashed curve generated defined by $\sigma(^{15}\text{N})/\sigma(^{12}\text{C}) = 1 - (1 - \sigma_n/\sigma_p)/15(1 + \sigma_n/\sigma_p)$ using $\sigma_n/\sigma_p = (1 - 0.8\xi)$, shown in Fig. 2, is a remarkably good approximation of the data, especially at the low Q^2 values of this experiment, where additional higher twist effects might be expected to play a role. This is particularly true if one averages over the quasielastic and Δ resonance regions [21]; in which case the resultant curve matches the Nachtmann-scaled extrapolation into the DIS region. This appears to perhaps be yet another manifestation

of quark-hadron duality, the fulfillment of which implies the marked absence or cancellation of higher twist effects [22]. That these higher twist, multiparton contributions appear to cancel nearly completely in the ratio is a noteworthy, if not unexpected, phenomenon at these values of Q^2 .

V. SUMMARY

We find that the (W, Q^2) dependence of ratios of electroproduction cross sections for $^{15}\text{N}/^{12}\text{C}$ and $^4\text{He}/^{12}\text{C}$ can be remarkably well described by a simple model based on superscaling in the quasielastic region and simple Fermi smearing in the nucleon resonance region, even at Q^2 values as low as 0.1 GeV^2 . Large oscillations in the ratios of $^4\text{He}/^{12}\text{C}$ that peaked near $W = 0.94, 1.23,$ and 1.5 GeV can be attributed to a difference in average Fermi momentum. In contrast, little structure is seen in the ratios of $^{15}\text{N}/^{12}\text{C}$, except for small effects in the $\Delta(1232)$ region and a decrease in the quasielastic region expected from the ratio of neutron to proton form

factors. The new data can be used to refine more detailed microscopic models of lepton-nucleon scattering in the nuclear medium.

Suitably averaged over W (as, for example, may occur naturally with the use of a wide-band neutrino beam), the ratios of $^{15}\text{N}/^{12}\text{C}$ and $^4\text{He}/^{12}\text{C}$ bear a strong resemblance to extrapolations of DIS models into the nucleon resonance region. This observation might be used to simplify predictions for neutrino oscillation experiments. It is also another indication of the applicability of the concepts of quark-hadron duality down to remarkably low values of Q^2 .

ACKNOWLEDGMENTS

We acknowledge the outstanding efforts of the Accelerator, Target Group, and Physics Division staffs that made this experiment possible. This work was supported by the U.S. Department of Energy, the Italian Istituto Nazionale di Fisica Nucleare, the U.S. National Science Foundation, the French Commissariat à l'Énergie Atomique, and the Korean Engineering and Science Foundation. The Southeastern Universities Research Association (SURA) operated the Thomas Jefferson National Accelerator Facility for the United States Department of Energy under Contract DE-AC05-84ER40150.

-
- [1] S. A. Kulagin, *Phys. Rev. D* **67**, 091301(R) (2003).
 [2] M. Hirai, S. Kumano, and T.-H. Nagai, *Phys. Rev. C* **76**, 065207 (2007).
 [3] J. Gomez *et al.*, *Phys. Rev. D* **49**, 4348 (1994).
 [4] M. Hirai, S. Kumano, and T.-H. Nagai, *Nucl. Phys. B, Proc. Suppl.* **139**, 21 (2005).
 [5] K. V. Dharmawardane *et al.* (CLAS Collaboration), *Phys. Lett. B* **641**, 11 (2006); P. E. Bosted *et al.* (CLAS Collaboration), *Phys. Rev. C* **75**, 035203 (2007).
 [6] C. D. Keith *et al.*, *Nucl. Instrum. Methods A* **501**, 327 (2003).
 [7] B. A. Mecking *et al.*, *Nucl. Instrum. Methods A* **503**, 513 (2003).
 [8] K. V. Dharmawardane, Ph.D thesis, Old Dominion University, 2004 (unpublished); Y. Prok, Ph.D thesis, University of Virginia, 2004 (unpublished).
 [9] L. Mo and Y.-S. Tsai, *Rev. Mod. Phys.* **41**, 205 (1969).
 [10] H. de Vries, *At. Data Nucl. Data Tables* **36**, 495 (1987).
 [11] T. W. Donnelly and I. Sick, *Phys. Rev. Lett.* **82**, 3212 (1999).
 [12] P. E. Bosted, *Phys. Rev. C* **51**, 409 (1995).
 [13] J. E. Amaro, M. B. Barbaro, J. A. Caballero, T. W. Donnelly, A. Molinari, and I. Sick, *Phys. Rev. C* **71**, 015501 (2005).
 [14] M. E. Christy and P. E. Bosted, arXiv:0712.3731 (2007).
 [15] P. E. Bosted and M. E. Christy, *Phys. Rev. C* **77**, 065206 (2008).
 [16] URL: www.jlab.org/~bosted/fits.html.
 [17] URL: clasweb.jlab.org/physicsdb/.
 [18] R. M. Sealock *et al.*, *Phys. Rev. Lett.* **62**, 1350 (1989).
 [19] B. Adeva *et al.*, *Phys. Rev. D* **58**, 112001 (1998).
 [20] O. Nachtmann, *Nucl. Phys.* **63**, 237 (1975).
 [21] F. E. Close and N. Isgur, *Phys. Lett. B* **509**, 81 (2001); F. E. Close and W. Melnitchouk, *Phys. Rev. C* **68**, 035210 (2003).
 [22] W. Melnitchouk, R. Ent, and C. Keppel, *Phys. Rep.* **406**, 127 (2005).